Structural consequences of ASR: an example on shear capacity

Joop A. den Uijl
Delft University of Technology, Faculty of Civil Engineering and Geosciences
P.O. Box 5048, 2600 GA Delft, The Netherlands
Niek Kaptijn
Bouwdienst Rijkswaterstaat, Afdeling Zuid, Tilburg, The Netherlands

Since the beginning of the nineties of the last century numerous viaducts in the Netherlands have been traced that suffer from ASR. Uniaxial tensile tests on cores drilled from the bridge decks sometimes showed a dramaticly low tensile strength. Since these decks are not provided with shear reinforcement, the question was raised whether the residual shear strength would still satisfy the requirements, the more so as in large parts of the decks mainly horizontally orientated cracks had developed.
To answer this question six beams, sawn from two 35 years old viaducts, were subjected to shear tests in the Stevin Laboratory at Delft University of Technology.
The observed crack development and shear strength could be explained by taking into consideration the influences of a longitudinal compressive stress due to the restraint of ASR induced expansion and an orientation dependent tensile strength.

Key words: concrete, ASR, tensile strength, shear, anisotropic material

1 Introduction

ASR related research could roughly be subdivided into two fields. First, the study of the chemical reactions involved and the conditions under which these reactions will occur are important for the prevention of ASR in new structures and to stop further deterioration in already affected structures. Second, the study of the effect of ASR on the strength and stiffness of affected structures is essential for the evaluation of the reliability of those structures. In the past the first mentioned field received most attention, but there is a growing interest in the second field that can be summarized under the heading 'Structural consequences of ASR'.

It is recognized that the development of local cracks due to ASR strongly depends on the boundary conditions. In the presence of a three-dimensional reinforcement cage the swelling of the confined part of the concrete is restricted and compressive stresses are generated, thus suppressing the development of internal cracks and preventing the structure from loosing bearing capacity. On the other hand, when in one direction no reinforcement has been applied, the ASR-induced swelling is not suppressed in that direction and more cracks will be developed perpendicular to it. The latter yields a reduction of particularly the uniaxial tensile strength in that direction. Since this strength reduction is orientation dependent an isotropic material behaviour will result.

The above-mentioned situation was observed in the decks of many flat slab bridges in The Netherlands. This raised the question whether the shear resistance, which in these cases fully depends on the tensile strength, would still satisfy the safety requirements. To answer this question it was decided to investigate in full-scale experiments the shear capacity of such bridge decks. In the beginning it was considered to load a complete bridge deck to failure, but this idea was rejected for two reasons. First, the time available for the preparation and execution of the tests would be very short because of the limited time that the highway could be closed. Second, it was wondered whether such a test would deepen the insight in the effect of ASR on the bearing mechanisms involved. Therefore the idea of testing a complete bridge deck was rejected and instead it was decided to cut beams from a deck, upon which the shear capacity would be tested under laboratory conditions.

On the basis of these tests a more rational conclusion could be drawn about the reliability of this type of structures affected by ASR. By these tests a better insight was gained in the bearing mechanism and last but not least the tests results can be used for the validation of numerical models that can simulate the structural consequences of ASR.

2 Experiments

2.1 Specimens

The first two beams, identified as ZB1 and ZB2, were sawn from the northern span of a three-span continuous slab viaduct (Figure1). The next four beams, identified as HS1 to HS4, came out the southern span of a similar viaduct (Figure 2). In both cases this was the most affected area of the deck as was found from tensile tests on drilled cores.

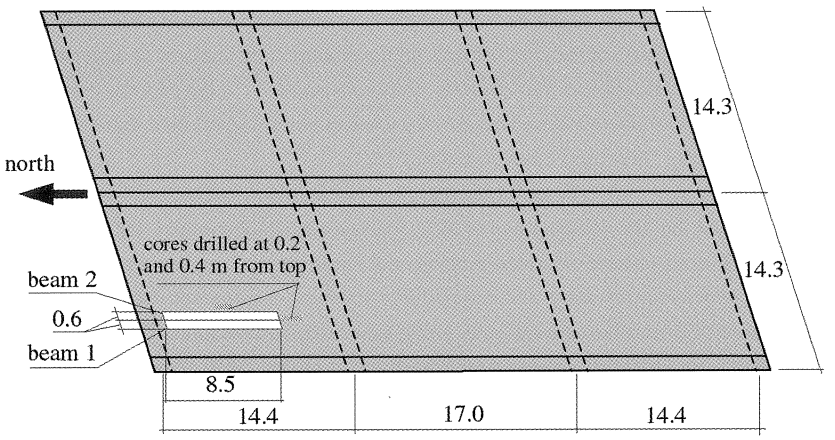

Figure 1. Position of beams and horizontal cores in north-west span of ZB-bridge

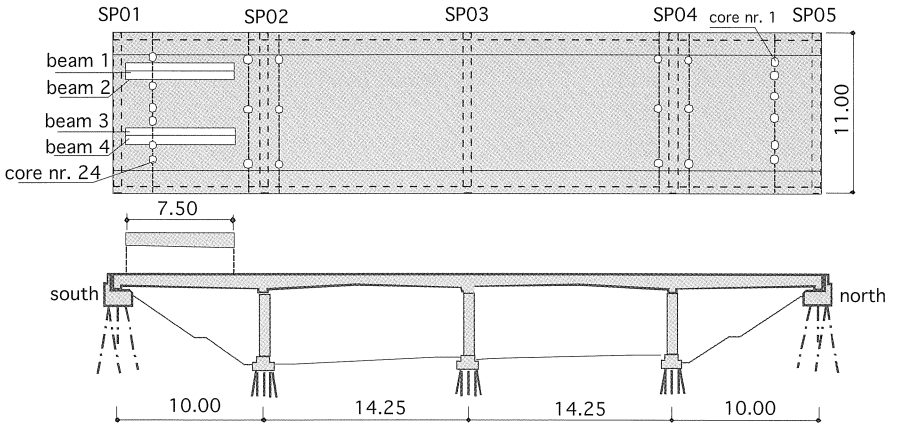

Figure 2. Position of beams and vertical cores in HS-bridge

An impression of the visible damage in this part of the ZB-bridge is given in Figure 3. The length of the ZB- and HS-beams was 8.5 and 7.5 m, respectively. The depth of the ZB-beams increased from 0.65 m at the north end to 0.75 m at the south end and in case of the HS-beams from 0.6 m at the south end to 0.75 m at the north end. Other dimensions are given in Table 1.

Figure 3. Visible damage due to ASR in north-west span of ZB-bridge

Table 1. Cross-sectional dimensions and reinforcement ratio of tested beams.

Test	b [mm]	d[1] [mm]	Internal bars[2]	External strips[3] [mm]	$\omega_{0,int}$[4] [%]	$\omega_{0,ext}$[4] [%]	$\omega_{0,tot}$[4] [%]
ZB1-North	600	620	$8Ø_k28$	-	1.32	-	1.32
ZB1-South	600	720	$8Ø_k28$	-	1.14	-	1.14
ZB2-North	600	640	$7Ø_k28$	-	1.12	-	1.12
ZB2-South	600	740	$7Ø_k28$	-	0.97	-	0.97
HS1-North	480	720	$2Ø_k25+2Ø_k22$	3x12x120	0.50	1.25	1.75
HS1-South	480	670	$2Ø_k25+2Ø_k22$	3x12x120	0.54	1.34	1.88
HS2-North	508	705	$2Ø_k25+2Ø_k22$	3x6x120	0.49	0.60	1.09
HS2-South	508	645	$2Ø_k25+2Ø_k22$	3x6x120	0.53	0.66	1.19
HS3-North	520	730	$2Ø_k25+2Ø_k22$	3x6x120	0.46	0.57	1.03
HS3-South	520	680	$2Ø_k25+2Ø_k22$	3x6x120	0.49	0.61	1.10
HS4-North	570	680	$2Ø_k25+2Ø_k22$	3x12x120	0.45	1.12	1.57
HS4-South	570	670	$2Ø_k25+2Ø_k22$	3x12x120	0.46	1.13	1.59

[1] Depth of section where inclined crack originated

[2] FeB 220, yield stress 220 MPa, diameter in mm

[3] Yield stress 410 MPa

[4] Reinforcement ratio related to dimensions of cross-section where inclined crack originated (int – internal, ext – external, tot – total)

2.1.1 Reinforcement

The reinforcement consisted of plain bars with 220 MPa nominal yield strength. Longitudinal and transverse bars were placed at the top and the bottom of the decks and only in the transverse beams over the supports and in the longitudinal edge beams vertical bars had been applied. The reinforcement ratios are given in Table 1.

Although in the ZB-tests diagonal cracks developed, the beams did not fail in shear, but their load capacity was limited by yielding of the steel. Moreover, the reinforcement ratio in the HS-beams was lower than in the ZB-beams and, finally, the ZB-beams had suffered more from ASR than the HS-beams. This meant that the HS-beams would probably fail in bending rather than in shear. Therefore the HS-beams were strengthened by means of steel strips glued to the bottom side over the entire beam length. In this way the bending resistance was increased more than the shear resistance. The dimensions of the strips are given in Table 1.

2.1.2 Concrete properties

When in a structure ASR is suspected a basic research is carried out, which includes the measurement of concrete strength and stiffness on vertically drilled 75 mm diameter cylinders. On the basis of the results of this basic research a more extensive investigation can be decided for. In case of HS-

viaduct this resulted in the strength values given in Table 2. The beams were sawn in the span that was limited by the end support and intermediate support at the south side.

Table 2. Compressive and tensile strength in bridge deck HS measured on 24 vertically drilled cylinders 75 mm (Visser et al., 1998b).

Type of Test	End support south	Intermediate supp. south	Intermediate supp. north	End support north	Average
Cube compressive	50.6 / 4[1)]	50.4 / 24	54.0 / 10	60.6 / 9	53.9 / 14
Splitting tensile ⊥[2)]	3.53 / 22	2.85 / 13	3.19 / 10	3.82 / 10	3.35 / 17
Splitting tensile //[3)]	3.45 / 11	3.16 / 5	3.37 / 14	4.21 / 14	3.55 / 16
Uniaxial tensile	1.02 / 48	0.84 / 45	0.89 / 26	1.61 / 17	1.11 / 42

[1)] *i* /*j* - average is *i* MPa and COV (coefficient of variation) is *j* %

[2)] ⊥ - splitting plane perpendicular to core axis

[3)] // - splitting plane parallel to core axis

The southern span close to the intermediate support had clearly suffered most from ASR. More striking, however, is the difference between the splitting tensile strength and the uniaxial tensile strength, for which with a 50 MPa cube strength would normally be expected 3.5 and 3.1 MPa, respectively. With respect to these values the splitting tensile strength is reduced by 10 to 20 %, whereas the uniaxial tensile strength is reduced by about 70 %. This difference can be understood by assuming that ASR damage results in disk like weakened spots. Due to the absence of vertical reinforcement these 'crack planes' will be orientated mainly horizontally, and a vertical cylinder may intersect some of these weakened planes; see Figure 4. Thus the tensile strength is not uniformly distributed over the height of the cylinder. This results in the observed difference between the uniaxial tensile strength, which reflects the strength of the weakest section, and the splitting tensile strength, which gives the strength at the section where the splitting force is applied. The average splitting strength perpendicular to the axis of the vertically drilled cylinders is somewhat lower than parallel to the axis, which is in accordance with the visual observation that the ASR crack planes were mainly horizontally orientated. Such anisotropy was also observed in unreinforced specimens by Larive (1998, 2000). Largest swelling and lowest tensile strength coincided with the casting direction. This was explained by the fact that due to sedimentation the concrete below large aggregate particles has the highest porosity, which facilitates the ASR. Moreover, disc like particles tend to be positioned horizontally, which enhances the forementioned effect. It is remarked that the reduction of the tensile strength in not unique for ASR-affected structures. Siemes et al (2002) ascribe such a reduction, which they have observed in many more structures, to a poor bond between aggregate and matrix due to the locally fluctuating water-cement ratio and various degrees of microcracking.

To quantify the anisotropy the tensile strength was measured in the principal directions of the ZB-viaduct (Visser et al., 1998a). In the northern span, from which the beams were sawn, the average

uniaxial tensile strength in vertical and in horizontal direction amounted to 0.6 MPa (COV 26 %, 15 tests) and 1.2 MPa (COV 28 %, 14 tests), respectively. The horizontally drilled cylinders were taken both in longitudinal and in transverse direction of the viaduct at two levels. The uniaxial tensile strength in longitudinal direction at 200 and 400 mm from the top was 1.08 MPa (COV 26 %, 4 tests) and 1.57 MPa (COV 8 %, 4 tests), respectively. In transverse direction no systematic difference between the uniaxial tensile strength at the two levels was found. In this case the average value was 1.03 MPa (COV 25 %, 6 tests).

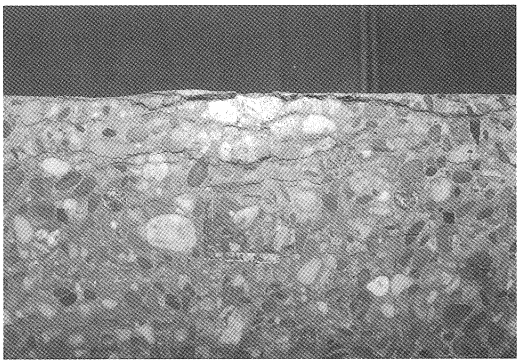

Figure 4. Horizontally oriented cracks at topside of ZB-beam

The influence of the load direction on the splitting tensile strength was much less than for the uniaxial tensile strength. The average of all splitting tensile tests was 2.83 MPa (COV 20 %, 21 tests). The compressive strength measured on cylinders with a height equal to the diameter was about 60 MPa. These values indicate that in the ZB-viaduct the reduction of both the uniaxial tensile strength and the splitting tensile strength was relatively more than in the HS-viaduct (see also Table 2).

2.2 Test execution and results

Both sides of the each beam were subsequently loaded until failure in a four-point-bending test with non-symmetric positioning of the loads; see Figure 5. The tested part of a beam was rein-

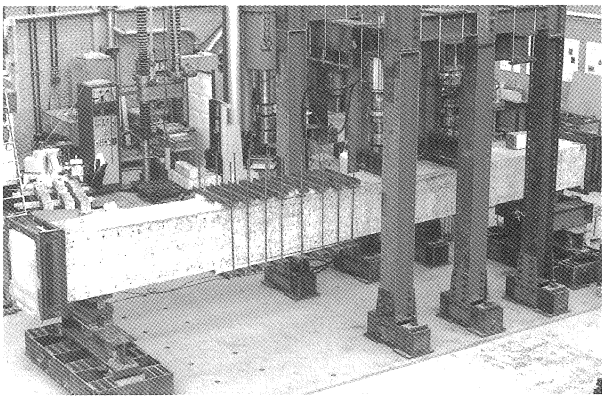

Figure 5. Four-point-bending test (already tested side was strengthened with clamps)

forced with steel clamps before the second test was done. The load was stepwise applied with two hand-operated jacks in about 2 hours. Loads, deflection and concrete strains along the shear span were automatically measured; see Figure 6. At each load step crack development was marked.

The main results of the experiments are summarized in Table 3. All ZB-beams failed in bending, although in ZB1 wide shear cracks had already developed when the reinforcement started to yield. The reinforcement ratio in ZB2 was less than in ZB1 (see Table 1), which explains why bending failure occurred at a lower load. All HS-beams failed in shear and no yielding of the reinforcement occurred. The average value of the ultimate shear stress of the ZB (except ZB2-south) and HS-beams is 1.34 and 1.49 MPa, respectively. The difference between these two values corresponds with the rate to which ASR had damaged the beams as was visually observed and also was confirmed by the results of the aforementioned tensile tests. The variation of the shear span to depth ratio between 2.5 and 4.5 did not influence the shear strength.

3 Analyses of the shear resistance

3.1 Mode of failure and shear strength without ASR

In case of rectangular beams without shear reinforcement flexural shear is normally the shear failure mechanism. Bending cracks will incline and develop towards the loading point until the compression zone fails. In the present case, however, failure was caused by shear tension, as was reflected by the initiation of inclined cracks at the neutral axis of the beam, see Figure 7. Without ASR the expected average load at shear failure is found according to Rafla (1971) from:

$$V_{u,theor} = \alpha_u d^{-0.25} \sqrt{f_{cc}} \sqrt[3]{\omega_0} bd \qquad (1)$$

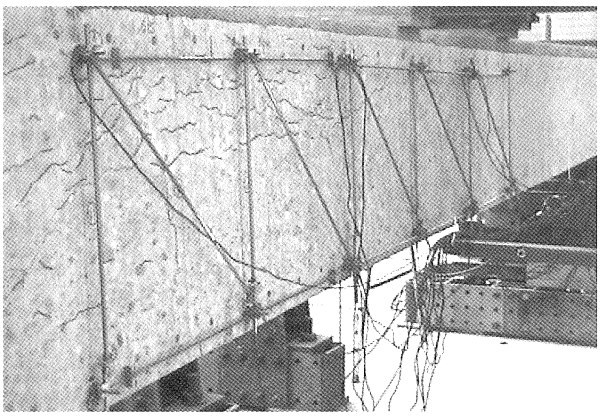

Figure 6. Deformation measurements along the shear span (visible cracks marked)

with $\alpha_u = 0.90 - 0.03\frac{a}{d}$ for $\frac{a}{d} \geq 3.5$

$$\alpha_u = 0.795 + 0.293\left(3.5 - \frac{a}{d}\right)^{2.5} \quad \text{for } 2.0 \leq \frac{a}{d} \leq 3.5$$

Substitution in Eq. (1) of the corresponding values from Table 1 and Table 2 and f_{cc} = 60 and 55 MPa for ZB and HS, respectively, yield the theoretical ultimate shear loads given in Table 3. The average ratio between the experimental and the theoretical strengths amounts to 0.60 (COV 9.5 %) for the ZB-beams and to 0.77 (COV 7.5 %) for the HS-beams. The difference between these two ratios can be ascribed to the combination of the facts that the ZB-beams did not fail in shear but in bending and that the ZB-beams suffered more from ASR than the HS-beams.

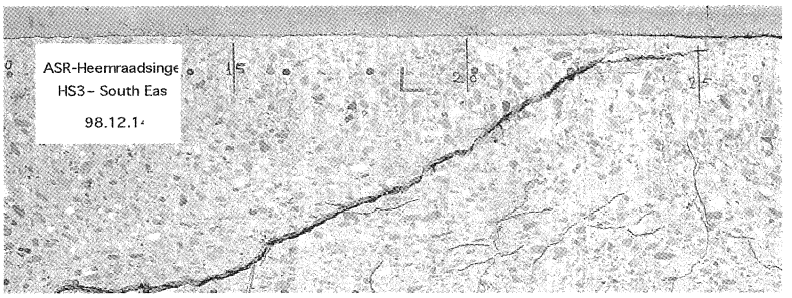

Figure 7. Beam end HS3-south after shear failure

Table 3. Ultimate shear force from tests and theory.

Test	$V_{u,test}$ [kN]	$\tau_{u,test}$ [1)] [MPa]	*a/d*	φ	$V_{u,theor}$ [2)] [kN]	$\frac{V_{u,test}}{V_{u,theor}}$	Failure mode [3)]
ZB1-North	354	1.42	3.07	21°	525	0.67	Bend./wide SC
ZB1-South	380	1.32	2.64	23°	675	0.56	Bend./fine SC
ZB2-North	330	1.29	2.97	30°	522	0.63	Bend./fine SC
ZB2-South	354	1.20	2.67	-	640	0.55	Bend./no SC
HS1-North	349	1.52	4.17	35°	421	0.83	Shear
HS1-South	330	1.54	4.48	32°	402	0.82	Shear
HS2-North	361	1.51	2.55	29°	507	0.71	Shear
HS2-South	321	1.47	2.79	28°	427	0.75	Shear
HS3-North	369	1.46	2.47	29°	541	0.68	Shear
HS3-South	350	1.49	2.65	28°	477	0.73	Shear
HS4-North	374	1.45	3.61	32°	470	0.80	Shear
HS4-South	380	1.49	3.88	25°	462	0.82	Shear

1) $\tau_{u,test} = 1.5\tau_{avg} = 1.5\frac{V_{u,test}}{bd}$ for a parabolic shear stress distribution over the beam depth

2) According to Eq. (1), (Rafla, 1971)

3) Bend. = bending; SC = Shear Crack

3.2 Influences of ASR on shear resistance

Two consequences of the occurrence of ASR will influence the structural behaviour under shear loading. First, compressive stresses may be developed in the concrete when the volume increase due to ASR is – partly – restrained by the reinforcement. With such a restraint the reduction of the strength, especially the tensile strength, is less than without restraint. Second, when the restraint is not available in all principal directions the tensile strength will depend on the orientation.

3.2.1 Influence of prestress

The influence of a longitudinal compressive stress σ_x on the shear resistance in case of diagonal tension failure follows from Mohr's circle. The magnitude of the ultimate shear stress τ_{xy} and the crack inclination φ is given by:

$$\tau_{xy} = \sqrt{f_{ct}^2 - f_{ct}\sigma_x} \tag{2}$$

$$\varphi = \arctan \frac{\tau_{xy}/f_{ct}}{1-\sigma_x/f_{ct}} \tag{3}$$

Figure 8b shows that the inclination of the crack plane decreases from 45° without prestress to 30° at a prestress that is in absolute value two times the tensile strength. In that case the ultimate shear stress is increased from the tensile strength to 1.73 times this value; see Figure 8a.

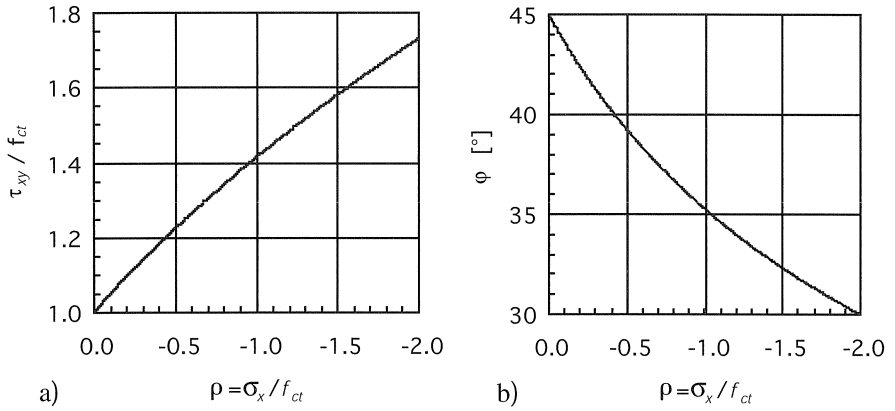

Figure 8. Ratio between the ultimate shear (a) stress and the crack inclination (b) as a function of the prestress ratio

Measurement of residual longitudinal steel strains in the HS-beams showed that the prestress in the concrete varied between -0.1 and -0.6 MPa with an average of -0.3 MPa. Thus, for an assumed tensile strength of 1.5 MPa the average ratio between prestress and tensile strength is -0.2 and the maximum is -0.4. With this maximum ratio the reduction of the crack inclination would not have been more than 5°; see Figure 8b. To explain the observed crack inclination (Table 3) from the influence of the prestress alone, a ratio between prestress and tensile strength of -2.0 is required. Then

the shear strength is 73 % higher than the tensile strength; see Figure 8a. The ultimate shear stress in the HS-tests measured 1.5 MPa; see Table 3. This would signify a tensile strength of 0.87 MPa and a prestress of -1.73 MPa. The latter is much more than derived from the steel strain measurements.

3.2.2 Influence of orientation dependent tensile strength

The anisotropic material behaviour is taken into account by considering a compressive prestress as an apparent tensile strength and vice versa. Or, in other words, the difference between the uniaxial tensile strength in vertical and in horizontal direction is added to the prestress from restrained ASR-expansion in horizontal direction, whereas the tensile strength is put equal to the uniaxial tensile strength in vertical direction.

Substitution of:

$$\sigma_x = \sigma_{x,res} - (f_{ct,90} - f_{ct,0}) \tag{4}$$

and $$f_{ct} = f_{ct,0} \tag{5}$$

in Eq. (2) and Eq. (3) yields:

$$\frac{\tau_{xy}}{f_{ct,90}} = \sqrt{\left(\frac{f_{ct,0}}{f_{ct,90}}\right)^2 - \frac{f_{ct,0}}{f_{ct,90}}\left(\frac{\sigma_{x,res} - (f_{ct,90} - f_{ct,0})}{f_{ct,90}}\right)} = \sqrt{\beta(1-\rho_{res})} \tag{6}$$

and $$\varphi = \arctan \frac{\tau_{xy}}{f_{ct,0} - \sigma_{x,res} + f_{ct,90} - f_{ct,0}} = \frac{\tau_{xy}/f_{ct,90}}{1-\rho_{res}} = \arctan \sqrt{\frac{\beta}{1-\rho_{res}}} \tag{7}$$

with $$\rho_{res} = \frac{\sigma_{x,res}}{f_{ct,90}} \tag{8}$$

In this way the anisotropic material is conceived as an isotropic material that is pre-compressed in one direction. Failure due to shear tension will occur when the principal tensile stress acting on the potential crack plane becomes equal to the isotropic tensile strength.

The aforementioned approach implicitly takes into account a tensile strength distribution in the anisotropic material that can be expressed as:

$$f_{ct,\varphi} = [\beta + (1-\beta)\sin\varphi] f_{ct,90} \tag{9}$$

To what extent this expression reflects the real situation cannot be judged on the basis of the material available.

3.3 *Discussion of analysis results*

For a number of prestress ratios (ρ_{res}) Eq. (6) and Eq. (7) are graphically displayed in Figure 9a and 9b, respectively. Some results that can be read from these graphs are summarized in Table 4. For a comparison with the test results, the observed inclination of the shear cracks is taken as a starting point. In the experiments on the HS-beams an average inclination of 30° (COV 10%, 8 results) was found and the average ultimate shear stress was 1.5 MPa; see Table 3. Further elements in the comparison are the vertical tensile strength and the prestress.

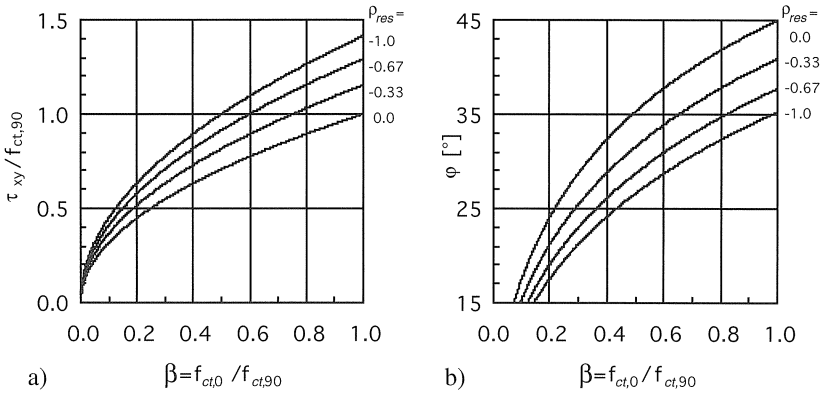

Figure 9. Ultimate shear stress (a) and inclination of failure plane (b) as a function of tensile strength ratio and prestress ratio

Table 4. Summary of analysis results.

φ [°]	ρ_{res} [2]	β [3]	$\tau_{xy}/f_{ct,90}$ [3]	$f_{ct,90}$ [4] [MPa]	$f_{ct,0}$ [5] [MPa]	$\sigma_{x,res}$ [6] [MPa]
25	-0.33	0.28	0.60	2.50	0.70	-0.83
30[1]	-2.00	1.00	1.73	0.87	0.87	-1.73
30	0.00	0.34	0.58	2.59	0.88	0.00
	-0.33	0.45	0.76	1.97	0.89	-0.65
	-0.67	0.56	0.95	1.58	0.88	-1.06
	-1.00	0.67	1.15	1.30	0.87	-1.30
35	-0.33	0.67	0.92	1.63	1.09	-0.54

[1] This row follows from Figure 8a and Figure 8b

[2] Assumed

[3] Read from Figure 9a and Figure 9b

[4] $f_{ct,90} = \tau_{xy,test}/(\tau_{xy}/f_{ct,90})$; $\tau_{xy,test}$ = 1.5 MPa

[5] $f_{ct,0} = \beta \cdot f_{ct,90}$

[6] $\sigma_{x,res} = \rho_{res} \cdot f_{ct,90}$

The average vertical uniaxial tensile strength in the region where the HS-beams were sawn was 0.93 MPa; see Table 2. This value agrees reasonably well with the vertical tensile strength found in the analysis, which appeared to depend only on the crack inclination. In horizontal direction the tensile strength had not been measured, but in the apparently more damaged ZB-viaduct the ratio between the vertical and horizontal tensile strength was 0.5. For this value of the tensile strength ratio, the analysis yields a prestress ratio of -0.5 and, hence, a prestress of -0.9 MPa, which is clearly higher than the aforementioned average value of -0.3 MPa, derived from steel strain measurements on HS-beams. With the latter prestress, which would mean a prestress ratio of -0.17, the analysis gives a tensile strength ratio of about 0.4, which contradicts the earlier assumption in this respect. Further investigation is required to determine whether this inconsistency is caused by a wrong estimation of e.g. the tensile strength ratio or the prestress or by shortcomings of the applied failure criterion.

An impression of the sensitivity of the calculated shear stress to the choice of various parameters can be found from Table 5. Assuming that the vertical tensile strength can be measured fairly, the prestress and the tensile strength ratio have been varied.

Table 5. Sensitivity of calculated shear strength to parameter choice

$f_{ct,0}$ [MPa]	$\sigma_{x,res}$ [MPa]	β	ρ_{res}	$\tau_{xy}/f_{ct,90}$	τ_{xy} [MPa]
0.9	-0.2	0.4	-0.09	0.66	1.48
		0.6	-0.13	0.82	1.23
0.9	-0.4	0.4	-0.18	0.70	1.57
		0.6	-0.27	0.86	1.29

The vertical tensile strength used in Table 5 corresponds to the average value measured in the HS-beams, where the average shear strength was found to be 1.5 MPa. It can be seen that the risk of overestimating the shear strength increases as the value for the prestress is put higher or the tensile strength ratio is put lower.

3.4 Practical application

In practice it will often hardly be possible to drill cores in horizontal direction in the most damaged part of a bridge deck. Therefore the following empirical relation is suggested for the estimation of the tensile strength ratio:

$$\beta = \sqrt{\frac{f_{ct,0}}{0.05 f_{cc} + 1}} \tag{10}$$

For the investigated cases this expression yields the values for the tensile strength ratio shown in Table 6. For the ZB-bridge the calculated uniaxial tensile strength in horizontal direction corresponds well with the average measured value on cores drilled in longitudinal direction at about mid-height; see section 2.1.2.

For the prestress ratio due to restraint ASR-expansion a relatively low value was adopted, which was two times higher for the ZB-bridge than for the HS-bridge because of the higher degree of ASR-attack and the higher reinforcement ratio in the ZB-bridge. It has been suggested to estimate the strain in the reinforcement on the basis of width of the visible gel filled cracks per unit length (ISE, 1992). However, in the present cases this did not yield reliable results.

Table 6. Ultimate shear stress from measured uniaxial tensile strength and cube strength and estimated prestress ratio.

Bridge	$f_{ct,0}$ [MPa]	f_{cc} [MPa]	β	$f_{ct,90}$ [MPa]	ρ_{res}	$\tau_{xy}/f_{ct,90}$	τ_{xy} [MPa]
ZB	0.6	60	0.39	1.54	-0.2	0.68	1.05
HS	0.93	50	0.51	1.82	-0.1	0.77	1.40

The ultimate shear stresses that are found from Figure 9a using the tensile strength ratios and the prestress ratios as start values, are shown in the last column of Table 6. In both cases the estimated shear stress is lower than the average value found in the tests (20 % and 7 % for ZB and HS, respectively).

It should be realized that uniaxial tensile tests on cores extracted from concrete that is damaged by ASR can only give a rough impression of the effective tensile strength because of the strong influence of local flaws on the tests results. More research is needed to establish reliable test methods for the – orientation dependent – tensile strength of the concrete in ASR affected structures.

4 Conclusions

The shear capacity of flat slab bridges without shear reinforcement that suffered from ASR has been studied. Six beams sawn from two bridges were loaded in bending until failure and a theoretical analysis was carried out, in which the effect of an orientation dependent tensile strength on the shear capacity was investigated. The following conclusions were drawn.

1. Due to the reduction of the tensile strength caused by ASR, the failure mechanism is of the shear tension type, whereas without ASR damage flexural shear failure would have been expected.
2. The average capacity in case of shear failure was 75% of the value that would have been expected when no ASR damage had occurred.
3. The crack inclination of about 30° could not be explained with the help of an ASR induced prestress alone.
4. By assuming an orientation dependent tensile strength the experimental findings could be made plausible. This assumption involves a failure criterion for an anisotropic material that needs further verification.

5. The shear resistance of a member without shear reinforcement that suffered from ASR can be estimated on the basis of the tensile strength in vertical direction, the tensile strength ratio and the prestress caused by partly restraint ASR expansion.

Acknowledgements

The authors gratefully acknowledge the financial support provided by Bouwdienst Rijkswaterstaat (Dutch Highway Authority) and and the fruitful discussions with the CUR Committee C106 'Structural -consequences of ASR' (Centre for Research and Recommendation in Civil Engineering, Gouda, The Netherlands).

References

- ISE, 1992. "Structural Effects of Alkali-Silica Reaction; Technical guidance on the appraisal of existing structures", The Institution of Structural Engineers, London, UK.
- Larive, C., 1998. "Combined Contribution of Testing and Modelling to the Understanding of the Alkali Reaction and its Mechanical Consequences (in French)". OA 28, Editor Laboratoire Central des Ponts et Chaussées, France.
- Larive, C., 2000. "Heterogeneity and Anisotropy in ASR-Affected Concrete. Consequences for Structural Assessment". In Proceedings 11th International Conference on Alkali-Aggregate Reaction in Concrete (Eds. M.A. Bérubé, B. Fournier, B. Durand). Québec City, June 2000, pp. 969-978.
- Rafla, K., 1971. "Empirical Equations for the Calculation of the Shear Resistance of Reinforced Concrete Beams (in German)". Strasse, Brücke, Tunnel 23, H. 12, pp. 311-320.
- Siemes, A.J.M, N. Han, J.H.M. Visser, 2002. "Unexpectedly low tensile strength in concrete structures". In present HERON.
- Visser, J.H.M., Siemes, A.J.M., Larbi, J.A., 1998a. "Prolonged Investigation of the Tensile Strength of Viaduct KW5 Zaltbommel (in Dutch)". TNO-rapport 98-BT-R0279, TNO Bouw, Delft, The Netherlands.
- Visser, J.H.M., Siemes, A.J.M., 1998b. "Investigation of the Uniaxial Tensile Strength of Viaduct Heemraadsingel (in Dutch)". TNO-rapport 98-BT-R1728, TNO Bouw, Delft, The Netherlands.

Notations

a = shear span
b = width of concrete section
d = depth of concrete section
f_{cc} = cube compressive strength
f_{ct} = concrete tensile strength

$f_{ct,0}$ = tensile strength for φ=0°

$f_{ct,90}$ = tensile strength for φ=90°

$V_{u,test}$ = ultimate shear force in test

$V_{u,theor}$ = ultimate shear force according to theory

β = tensile strength ratio = $f_{ct,0} / f_{ct,90}$

φ = inclination of crack plane with respect to longitudinal axis

ρ = prestress ratio = σ_x / f_{ct}

ρ_{res} = ratio between prestress due to restraint ASR-expansion and tensile strength in corre sponding direction = $\sigma_{x,res} / f_{ct,90}$

σ_x = normal stress in longitudinal direction (compression is negative)

$\sigma_{x,res}$ = normal stress in longitudinal direction due to restraint ASR-expansion

τ_{xy} = ultimate shear stress

$\tau_{u,test}$ = ultimate shear stress in test

ω_o = reinforcement ratio in %

COV = coefficient of variation